

PAPER • OPEN ACCESS

## Behavior and Mobility of U Series Radionuclides during Gibbsite Processing, Abu Thor Locality, Sinai, Egypt

To cite this article: R. M. Attia *et al* 2024 *J. Phys.: Conf. Ser.* **2830** 012026

View the [article online](#) for updates and enhancements.

You may also like

- [The U-series dating of \(biogenic\) carbonates](#)  
C Hillaire-Marcel
- [An investigation into the upward transport of uranium-series radionuclides in soils and uptake by plants](#)  
D Pérez-Sánchez and M C Thorne
- [The influence of building material structure on radon emanation](#)  
Predrag Kuzmanovi, Bojan Miljevi, Nataša Todorovi *et al.*



**ECS** The Electrochemical Society  
Advancing solid state & electrochemical science & technology

**ECS UNITED**

**247th ECS Meeting**  
Montréal, Canada  
May 18-22, 2025  
*Palais des Congrès de Montréal*

**Showcase your science!**

**Abstracts due December 6th**

# Behavior and Mobility of U Series Radionuclides during Gibbsite Processing, Abu Thor Locality, Sinai, Egypt

R. M. Attia<sup>1</sup>, N. M. Harpy<sup>1</sup> and H. K. Sarhan<sup>1</sup>

<sup>1</sup>Nuclear Materials Authority, P.O. Box 530, El-Maadi, Cairo, Egypt

[chredamohamed@yahoo.com](mailto:chredamohamed@yahoo.com)

**Abstract.** Gamma spectrometry was employed to measure the natural activity of radionuclides using High purity germanium detector during the leaching of gibbsite sample from Abu Thor locality using three different organic agents. Among these agents, EDTA exhibited the lowest leaching efficiency for <sup>238</sup>U, approximately 21%, while oxalic and citric acids achieved efficiencies of 42.77% and 32.44%, respectively. The leaching process revealed that the leaching efficiency of <sup>234</sup>U and <sup>232</sup>Th were higher than that of <sup>238</sup>U, <sup>230</sup>Th, and <sup>235</sup>U. Additionally, the radionuclides <sup>226</sup>Ra, <sup>214</sup>Pb, and <sup>214</sup>Bi were predominantly found in the residue of the three organic agents. The oxalic acid residual sample shows the highest ratios for <sup>230</sup>Th/<sup>238</sup>U, <sup>226</sup>Ra/<sup>238</sup>U, and <sup>226</sup>Ra/<sup>230</sup>Th ratios, all exceeding 1, with values of 1.33, 1.6, and 1.22, respectively. Therefore, the <sup>226</sup>Ra/<sup>238</sup>U ratio is deemed superior for studying the behavior and mobility of U.

**Keywords:** HP-Ge spectrometry; U and Th series; organic leaching; EDTA, Oxalic acid and Citric acid

## 1. Introduction

Naturally U and Th are ubiquitous within rocks, ground and sediment. The composition of natural uranium includes isotopes <sup>238</sup>U, <sup>235</sup>U, and <sup>234</sup>U, with percentages of 99.284%, 0.711%, and a trace amount of 0.0055%, respectively [1]. Thorium is naturally present in sediment in the forms of <sup>232</sup>Th and <sup>234</sup>Th, the latter being a progeny of <sup>238</sup>U [2]. Under secular equilibrium the activity ratios between <sup>238</sup>U parents and its daughter nuclide is unity [3], however, this ratio is deformed from unity due to chemical and physical fractionation [4]. <sup>232</sup>Th is less soluble than <sup>238</sup>U and is typically found mostly in secular equilibrium with its progeny, including <sup>228</sup>Ra, <sup>212</sup>Pb, <sup>212</sup>Bi, and <sup>208</sup>Tl. Disequilibrium arises from geochemical processes, where they result in mobility or accumulation of each of them at a rate depend on the characteristic of the occurred disturbance [5] and relative to the daughter half-life [3]. Among almost important factors leading to disequilibrium are weathering processes at the surface of the earth, radionuclides chemically fractionated resulting from the variability in their chemical characteristics in U series, diffusion of radon gas isotopes and physical fractionation through radioactive decay (alpha recoil) [2]. The disequilibrium system of <sup>234</sup>U/<sup>238</sup>U provides a wide range of purpose for studying



different Earth-surface processes. These include inquiry the development of weathering profiles, erosion over time and examining sediment transfer processes across river catchments [3].

In oxidizing conditions, uranium typically exists in the hexavalent  $U^{+6}$  state, predominantly as  $UO_2^{2+}$  with notable mobility forming soluble carbonate and phosphate complexes. Conversely, under geochemical conditions where dissolved oxygen is depleted, uranium adopts the  $U^{4+}$  state creating insoluble complexes with inorganic ligands (hydroxides, phosphates and hydrated fluorides) [6]. Radium exists in a divalent state and displays moderate solubility in natural waters. It has the potential to precipitate in various forms, such as sulphate, carbonate, and chromate salts. The decay series of uranium, thorium, and actinium are the principal origin of radium isotopes ( $^{228}Ra$ ,  $^{226}Ra$ ,  $^{224}Ra$  and  $^{223}Ra$ ) [7]. Radium can enter into groundwater through aquifer dissolution, desorption from the rock or sediment surfaces, and expulsion from minerals during radioactive decay [8]. In the absence of any separation between radionuclide mothers and daughters for a period of 8000 years, the geochemistry of  $^{226}Ra$  is entirely governed by  $^{230}Th$  [9].

Natural thorium is exclusively composed of the isotope  $^{232}Th$ , serving as the origin nuclide in the thorium decay chain. Thorium occurs solely in the tetravalent oxidation state in solutions, exhibiting very slight solubility in nearly all watery environments due to  $Th^{4+}$  rise ionic potential [10], on the other hand any amount of it can be dissolved is adsorbed and precipitated as a result of its ionic potential of tetravalent state [11].  $^{40}K$  is one of the natural radioactive isotopes, occurring in different rocks such as metamorphic, magmatic, feldspathoids and micas, on the other hand it can be formed in sedimentary environments related to its presence in potash feldspars and plagioclase [11]. The primary organic acids generated by fungi in bioleaching for the purposes of dissolving uranium from uranium-bearing ores are citric and oxalic acid [12]. In the bioleaching process, fungi possess the capability to extract uranium from its ores by producing organic acids, namely citric and oxalic acids [13]. Both naturally-occurring and artificially produced ligands, including citrate, oxalate, fulvic acid, humic acid and EDTA are recognized for their ability to create robust aqueous complexes with  $U^{+6}$ . This phenomenon can markedly increase the mobility of  $U^{+6}$  [14-15].

Extensive research has been conducted on ethylenediaminetetraacetic acid (EDTA) as a chelating agent for metals. Studies have demonstrated the extraction of zinc, cadmium, copper, and lead in a 1:1 ratio through metal-EDTA complexes from polluted soils [16-17]. Aqueous alkaline solutions containing EDTA have proven effective in dissolving  $Ba(Ra)SO_4$  and extracting  $^{226}Ra$  from uranium tailings [18]. At pH 5.5 to 6.9 with the disodium salt by (EDTA), an anion complex of radium is formed, below pH 4.5, no complex forms, while at pH 7-8 no free radium ions in solution can be detected [19]. This work aims to follow the radionuclides mobilization during different stages of gibbsite ore processing and detect the capability of various organic acids in uranium leaching.

## 2. Experimental and Analytical Approaches

### 2.1 Characterization of the Ore

The Um Bogma Formation at Abu Thor is visible 40 kilometers to the east of Abu Zinema City in Sinai. This geological formation exhibits an unconformable overlay on the Adedia Formation, consisting of shales and sandstones. Simultaneously, it is covered by the non-fossiliferous bleached sandstones of the Abu Thora Formation in an unconformable manner. The examined gibbsite sample was gathered from Abu Thor locality, subjected to crushing, and ground to roughly (-60) mesh. Approximately 5 grams of the gibbsite sample underwent further grinding to -200 mesh for major oxides chemical analyses, employing the [20] method. The gravimetric determination of the loss on ignition (L.O.I) was carried out at 1000 °C. X-ray fluorescence technique was used for the trace elements determination in the Laboratories of Nuclear Materials Authority (NMA).

The determination of  $^{238}\text{U}$ ,  $^{235}\text{U}$ ,  $^{234}\text{U}$ ,  $^{230}\text{Th}$ ,  $^{226}\text{Ra}$ , and  $^{232}\text{Th}$  were conducted Hyper Pure Germanium detector (HPGe) with a packed time ranging between 20 and 24 hours. The HPGe detector features has an efficiency of approximately 60% relative to of a 3"  $\times$  3" NaI (Tl) crystal efficiency, a resolution of 2.3 keV, and a peak/Compton ratio of 56:1 at the 1.33 MeV gamma transition of  $^{60}\text{Co}$ . The framework underwent energy calibration, displaying gamma photopeaks within the range of 46 keV to 3000 keV. Efficiency calibration was carried out using three established reference materials for U, Th, and K activity measurements: RGU-1, RGTh-1, and RGK-1, as provided by (IAEA) in 1987 [21-22].

## 2.2 Leaching process

The samples measured using Hyper Pure Germanium detector (HPGe) were transferred from the ductile container and divided into exemplary sections for dissolution tests. Nonconventional organic agents, specifically citric, oxalic, and ethylenediaminetetraacetic acid, were employed in the leaching process with magnetic stirrers for agitation. Each leaching experiment involved agitation about 50 grams of the finely grind sample with 150 ml of each acid concentration at 200 gm/l for 1 hour at ambient temperature. Following the dissolution, the sample slurry was filtered, washed multiple times with distilled water, and then adjusted to a volume of 250 ml. The remaining residuals were dried at 110 °C, Both the leachates and residuals were subjected to measurements for the aforementioned radionuclides using the Hyper Pure Germanium detector (HPGe).

The determination of radionuclide leaching efficiency was conducted through the following equation:

$$\text{Leaching Efficiency (\%)} = \frac{\text{Activity concentration in the leachate}}{\text{Activity concentration in the original sample}} \times 100$$

## 3. Results and Discussions

### 3.1 Characteristics of the studied sample

The major oxide chemical analysis presented in Table 1 reveals that the predominant constituents of the examined gibbsite sample are  $\text{SiO}_2$ ,  $\text{Al}_2\text{O}_3$ ,  $\text{Fe}_2\text{O}_3$ ,  $\text{MnO}$ ,  $\text{CaO}$ ,  $\text{MgO}$ , and  $\text{SO}_3$ , with respective concentrations of 15.3%, 17.4%, 17.6%, 9.68 %, 3.5%, 6.0%, and 3.53%. The chemical analysis of Trace elements as shown Table 1, indicate that the main components of the studied gibbsite sample are Zn, Zr, Pb and Ni with assay 6811, 6762, 3879 and 1305 ppm respectively. On the other hand, chemical index of alteration (CIA) was calculated from the major oxides of this sample which used as an index of major element diversity resulting from alteration processes and transmutation of feldspars, volcanic glass and other labile components to clay minerals according to the following equation:

$$\text{CIA} = [\text{Al}_2\text{O}_3 / (\text{Al}_2\text{O}_3 + \text{K}_2\text{O} + \text{Na}_2\text{O} + \text{CaO})] \times 100$$

Worldwide average CIA values for shale vary from about 70 and 75; 50 for fresh granites [23], while ultimate weathering values may reach to 100 [24]. In the studied gibbsite sample CIA value is 71.48 which indicate moderately weathered terrains.

**Table 1.** Summarizes the chemical analysis of the gibbsite sample.

Major oxides	$\text{SiO}_2$	$\text{Al}_2\text{O}_3$	$\text{TiO}_2$	$\text{Fe}_2\text{O}_3$	$\text{CaO}$	$\text{MgO}$	$\text{Na}_2\text{O}$	$\text{K}_2\text{O}$	$\text{MnO}$	$\text{P}_2\text{O}_5$	$\text{CuO}$	$\text{Cl-}$	$\text{SO}_3$	L.O.I	CIA (%)
Wt., %	15.32	17.4	0.31	17.6	3.5	6	2.5	0.82	9.68	1.3	1.28	0.67	3.53	19.6	71.84
Trace elements	Cr	Ni	Zn	Zr	Rb	Y	Ba	Pb	Sr	Ga	V	Nb			
ppm	u.d	1305	6811	6762	148	u.d	258	3879	695	635	84	220			

(u.d: Under Detection)

### 3.2 Radiometric measurements

Table 2 provides the activity concentrations of Th and U radionuclides in the examined gibbsite sample, including several calculated ratios. The isotopic ratios of various radionuclides offer insights into the processes occurring in these rock varieties.

**3.2.1 Original ore Sample:** The activity ratio of  $^{232}\text{Th}/^{238}\text{U}$  in the original ore sample is 0.03, this ratio deviates from the typical values found in the Earth's crust, which range from 3 to 4 [8, 25] suggesting an enrichment of uranium in this sample. The  $^{234}\text{U}/^{238}\text{U}$  activity ratios (ARs) are 0.59 less than 1, implying a discriminatory leaching of  $^{234}\text{U}$  compared to  $^{238}\text{U}$  from the rock, which can be attributed to the prevailing oxidizing conditions [8, 26]. The  $^{226}\text{Ra}/^{238}\text{U}$  and  $^{230}\text{Th}/^{238}\text{U}$  isotopic ratios are 1.14 and 1.19, respectively close to 1 suggest equilibrium between  $^{238}\text{U}$  with its daughter  $^{226}\text{Ra}$  and  $^{230}\text{Th}$ . The  $^{226}\text{Ra}/^{230}\text{Th}$  activity ratio is close to unity (0.96), indicating equilibrium conditions that have persisted for a maximum time period of 8 thousand years. The  $^{238}\text{U}/^{235}\text{U}$  activity ratio is 21.69, falling within the natural ratio range (21.7). So, from all the calculated ratios suggest that the two radionuclides mobility are nearly identical.

**3.2.2. Leachate analysis:** After subjecting the samples to leaching experiments involving various acids, the concentration of radionuclides in the leachate was quantified using gamma-ray spectroscopy. The results, depicting the activity of radionuclides such as  $^{238}\text{U}$ ,  $^{234}\text{U}$ ,  $^{235}\text{U}$ ,  $^{234}\text{Th}$ ,  $^{230}\text{Th}$ ,  $^{226}\text{Ra}$ ,  $^{232}\text{Th}$ ,  $^{214}\text{Pb}$ ,  $^{214}\text{Bi}$  and  $^{40}\text{K}$ , are presented in Table 2 and Figure 1. Notably, EDTA demonstrated the least leaching efficiency for  $^{238}\text{U}$ , approximately 21%, while oxalic and citric acids achieved efficiencies of 42.77% and 32.44%, respectively. An important observation is the consistent leachability of  $^{235}\text{U}$  and  $^{238}\text{U}$  across all leaching agents. On the other hand, the leaching of  $^{234}\text{U}$  varied with respect to  $^{238}\text{U}$  and  $^{235}\text{U}$  across all leaching agents. Notably, EDTA demonstrated the highest leaching efficiency for  $^{234}\text{U}$ , approximately 76.89 %, while oxalic and citric acids achieved efficiencies of 73.6 % and 66.25 %, respectively.

Hence, it's observed that the transfer proportion of the lighter isotope of uranium exceeded that of the heavier ones. This suggests that  $^{234}\text{U}$  exhibits higher mobility compared to its precursors and daughters across all leaching agents. Research focused on developing the conceptual model of oxidative isotope fractionation of  $^{234}\text{U}$  indicates that  $^{234}\text{Th}$ , a daughter nuclide of  $^{238}\text{U}$ , tends to be pushed into rock matrix areas due to alpha-recoil. This movement results in the accumulation of oxygen atoms around the  $^{234}\text{Th}$  nuclei [27]. The high energy released during decay can elevate the oxidation potential at the terminus of the  $^{234}\text{Th}$  recoil trajectory. Consequently,  $^{234}\text{U}$  may be activated into the more stable hexavalent oxidation state. This phenomenon occurs alongside the presence of  $^{238}\text{U}$  existing in the fourth oxidation state within rock-forming minerals.

The elevation of the  $^{234}\text{U}/^{238}\text{U}$  isotopic ratio to larger than 1 in EDTA leachate solutions (2.18) signifies the lowest efficiency in leaching of  $^{238}\text{U}$  (20.72%) and the higher efficiency in leaching  $^{234}\text{U}$  (76.89%). In contrast, decrease in the  $^{234}\text{U}/^{238}\text{U}$  activity ratio  $< 1$  was noted across all leaching agent residuals (EDTA 0.55, Oxalic acid 0.34, and Citric acid 0.38), indicating the  $^{238}\text{U}$  migration into the residual. The remarkably low leaching efficiency for  $^{230}\text{Th}$ ,  $^{214}\text{Pb}$ , and  $^{214}\text{Bi}$  across all leaching agents ranged from 12.37% to 14.78%, from 0.14% to 3.67%, and from 0.10% to 4.38%, respectively. The immobilization of  $^{230}\text{Th}$ ,  $^{214}\text{Pb}$ , and  $^{214}\text{Bi}$  may be attributed to the high iron oxide content (17.6%) and manganese oxide content (9.68%) [26, 28]

The radionuclides  $^{226}\text{Ra}$ ,  $^{214}\text{Pb}$ , and  $^{214}\text{Bi}$  were predominantly found in the residue of the three organic agents, suggesting an association with radium sulfate or to some extent insoluble mineral phases such as refractory oxides and alumina silicates. There was a notable high-efficiency leaching of  $^{232}\text{Th}$  by the leaching agents EDTA (88.9%) and Oxalic acid (81.98%), the enhanced leaching efficiency of

$^{232}\text{Th}$  may be realized to its faint activity and its adsorption on soluble organic matter [26]. The activity concentration of  $^{40}\text{K}$  in the residual material for all leach agents and leach liquor of the leach agents (EDTA and Oxalic acid) was found to be higher than that of the original rock, as shown in Figure 4. This abnormal increase in potassium values may be related to the occurrence of Pb (3879 ppm) as a component of the original sample, which could cause self-attenuation effects on the radionuclides in the original sample. So, the absence of Pb in the leachate results in a decrease in self-attenuation, allowing for the measurement of gamma activities in the inner grains. Another effective factor is the increments in the ratio of clay minerals in the residual relative to the pregnant solution and ore sample.

Tables 2, along with Figure 2 histograms, illustrate the comparison between the activity of radionuclides, including  $^{238}\text{U}$ ,  $^{234}\text{U}$ ,  $^{235}\text{U}$ ,  $^{234}\text{Th}$ ,  $^{230}\text{Th}$ ,  $^{226}\text{Ra}$ ,  $^{232}\text{Th}$ ,  $^{214}\text{Pb}$ ,  $^{214}\text{Bi}$ , in the original sample and the resulting residual from three leaching agents. It is observed that the activity concentrations of most radionuclides in the residual, especially  $^{40}\text{K}$ , are higher than those present in the original rock. Furthermore, the total activity concentrations for various radionuclides in both the pregnant solution and residual material surpass the activity levels detected in the original sample. This observation is attributed to the impact of acid solutions utilized during the leaching experiments, which likely facilitated the cleaning of the residual grain surface. Consequently, the cleaning process permits the measurement of gamma activities in the inner grains, as discussed in previous studies [8, 29].

Figure 3 histogram illustrates the comparison of several calculated isotopic ratios, including  $^{234}\text{U}/^{238}\text{U}$ ,  $^{230}\text{Th}/^{238}\text{U}$ ,  $^{226}\text{Ra}/^{238}\text{U}$ , and  $^{226}\text{Ra}/^{230}\text{Th}$ , in the original sample and resulting residual from three leaching agents. The ratio  $^{234}\text{U}/^{238}\text{U}$  is consistently below 1, indicating the lowest ratio for the original and all residual samples, ranging from 0.59 to 0.34. The highest leaching efficiency for  $^{238}\text{U}$  is observed with Oxalic acid. Consequently, the Oxalic acid residual sample exhibits the highest ratios for  $^{230}\text{Th}/^{238}\text{U}$ ,  $^{226}\text{Ra}/^{238}\text{U}$ , and  $^{226}\text{Ra}/^{230}\text{Th}$ , all exceeding 1, with values of 1.33, 1.6, and 1.22, respectively. Therefore, the  $^{226}\text{Ra}/^{238}\text{U}$  ratio is deemed superior for studying the behavior and mobility of U.

**Table 2.** Activity and isotopic ratios of radionuclides in original, pregnant solution and residual samples by EDTA, Oxalic Acid and Citric acid.

Radionuclide	EDTA			Residual (Bq/kg)	Oxalic Acid			Residual (Bq/kg)	Citric acid		
	Original (Bq/kg)	Leachate (Bq/l)	Leachability (%)		Leachate (Bq/l)	Leachability (%)	Residual (Bq/kg)		Leachate (Bq/l)	Leachability (%)	Residual (Bq/kg)
<b><math>^{238}\text{U}</math> series</b>											
$^{234}\text{Th}$	4263.5	865.7	20.31	3771.8	1823.4	42.77	3629.4	1374.5	32.24	4614.3	
$^{234}\text{mPa}$	4262.3	900.6	21.13	3671.5	1868.2	43.83	3561.6	1374.08	32.24	5045.7	
<b>Average</b>	<b>4262.9</b>	<b>883.1</b>	<b>20.72</b>	<b>3721.7</b>	<b>1845.8</b>	<b>43.3</b>	<b>3595.5</b>	<b>1374.08</b>	<b>32.24</b>	<b>4829.9</b>	
$^{234}\text{U}$	2506.9	1927.7	76.89	2038.6	1845.2	73.6	1381.9	1660.9	66.25	1835.4	
$^{230}\text{Th}$	5080.6	751.03	14.78	4205.4	628.6	12.37	4448.9	686.7	13.51	4811.2	
$^{226}\text{Ra}$	4870.8	106	2.2	4583.1	75.4	0.02	5418.1	313.6	6.56	5875.8	
$^{214}\text{Pb}$	4020.8	147.8	3.67	3059.4	51.4	1.28	4163.7	5.78	0.14	4836.9	
$^{214}\text{Bi}$	3963.7	173.4	4.38	2950.3	69.7	1.76	4008.1	3.89	0.10	4705.1	
<b><math>^{235}\text{U}</math> series</b>											
$^{235}\text{U}$	196.6	40.41	20.56	171.13	84.76	43.11	165.50	63.07	32.09	222.5	
<b><math>^{232}\text{Th}</math> series</b>											
$^{228}\text{Ac}$	36.8	32.1	88.5	57.64	33.63	93.68	53.88	5.4	14.88	54.4	
$^{208}\text{Tl}$	35.9	31.1	86.6	33.77	25.226	70.27	uld	uld	uld	24.3	
<b>Average</b>	<b>36.1</b>	<b>31.6</b>	<b>88.9</b>	<b>26.63</b>	<b>29.43</b>	<b>81.98</b>	<b>53.88</b>	<b>5.4</b>	<b>14.96</b>	<b>39.4</b>	
$^{40}\text{K}$	238.8	1028.50		856.59	1018.35		714.92	220.1		736.3	
$^{238}\text{U}/^{235}\text{U}$	<b>21.69</b>	<b>21.85</b>		<b>21.75</b>	<b>21.78</b>		<b>21.59</b>	<b>21.79</b>		<b>21.71</b>	
$^{234}\text{U}/^{238}\text{U}$	<b>0.59</b>	<b>2.18</b>		<b>0.55</b>	<b>1</b>		<b>0.34</b>	<b>1.21</b>		<b>0.38</b>	
$^{230}\text{Th}/^{238}\text{U}$	<b>1.19</b>	<b>0.85</b>		<b>1.13</b>	<b>0.34</b>		<b>1.33</b>	<b>0.50</b>		<b>1.00</b>	
$^{226}\text{Ra}/^{238}\text{U}$	<b>1.14</b>	<b>0.12</b>		<b>1.23</b>	<b>0.04</b>		<b>1.6</b>	<b>0.23</b>		<b>1.22</b>	
$^{226}\text{Ra}/^{230}\text{Th}$	<b>0.96</b>	<b>0.14</b>		<b>1.09</b>	<b>0.12</b>		<b>1.22</b>	<b>0.46</b>		<b>1.22</b>	
<b>U (ppm)</b>	<b>343.78</b>	<b>71.22</b>		<b>263.45</b>	<b>148.86</b>		<b>247.78</b>	<b>110.81</b>		<b>389.5</b>	

Th (ppm)	8.93	7.82	6.59	7.28	10.26	1.34	9.74
----------	------	------	------	------	-------	------	------

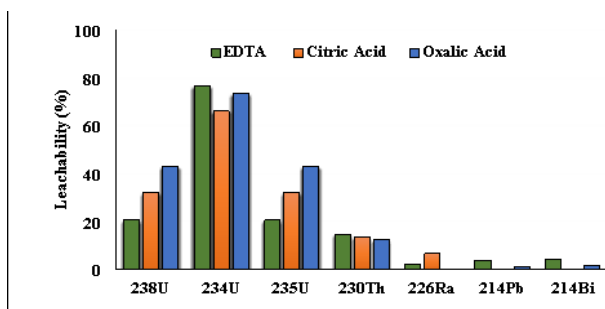


Figure 1. Leaching efficiency (%) of different radionuclides by different organic agents.

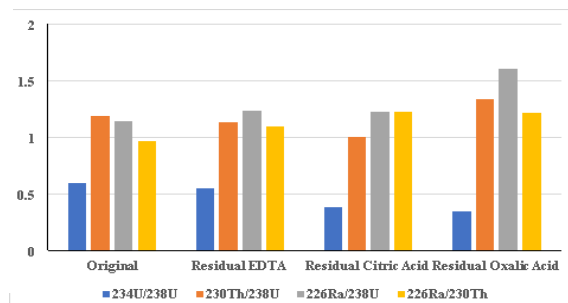


Figure 3. Variations of the  $^{234}\text{U}/^{238}\text{U}$ ,  $^{230}\text{Th}/^{238}\text{U}$ ,  $^{226}\text{Ra}/^{238}\text{U}$  and  $^{226}\text{Ra}/^{230}\text{Th}$  activity ratios in original, and residuals.

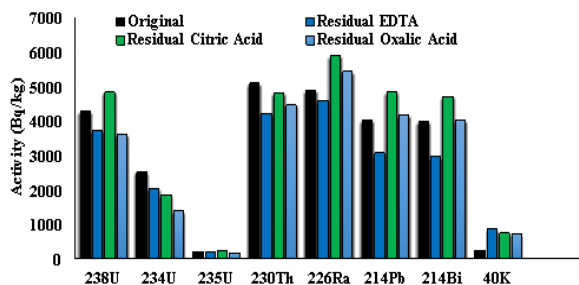


Figure 2. Activity concentration (Bq/kg) of different radionuclides in original and residuals.

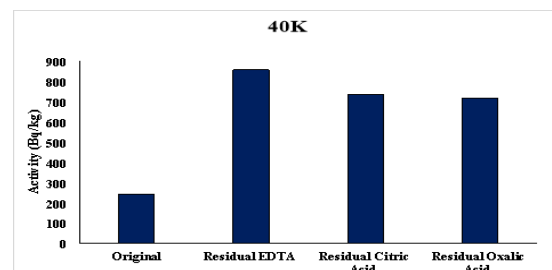


Figure 4. Activity concentration (Bq/kg) of  $^{40}\text{K}$  in original and residuals.

#### 4. Conclusions

Gibbsite rock sample was collected from Abu Thor locality, Sinai, Egypt, to study the leaching behavior and mobility of radionuclides in U-series. An HPGe detector was employed to measure the activity of U-series radionuclides in the ore sample, the pregnant solution resulting from different organic agents, and its residual phases. The data clarified that the leaching of  $^{234}\text{U}$  is greater than  $^{238}\text{U}$  and  $^{235}\text{U}$  across all leaching agents due to the alpha recoil effect. In addition to, the leachability percentage of  $^{235}\text{U}$  closely matched that of  $^{238}\text{U}$  across all leach liquors, maintaining a natural ratio value of 21.7. On the other hand, low leaching efficiency for  $^{230}\text{Th}$ ,  $^{214}\text{Pb}$ , and  $^{214}\text{Bi}$  in all leaching agents may be realized to the high iron and manganese oxide content. Radium series radionuclides ( $^{226}\text{Ra}$ ,  $^{214}\text{Bi}$ ,  $^{214}\text{Pb}$ ) exhibited low solubility in all tested organic agents' solutions, leading to their concentration in the residual samples. Consequently, the  $^{226}\text{Ra}/^{238}\text{U}$  ratio was identified as superior for studying the behavior and mobility of

U. Additionally, the summation of activity for various radionuclides in pregnant solutions and residuals with the studied organic agents exceeded the activity in the original ore samples due to the effects of leaching process which result in cleaning of the residual grain surface and hence permits freeing gamma rays to be detectable.

## References

- [1] Elsayeda A, Husseina M, El-Mongyb S, Ibrahima H, Shazlyc A and Abdel-Rahman M 2021 *Radiochem.* 63 627–634. DOI: 10.1134/S1066362221050118
- [2] Abdul J, Umme F, Amy L and Cynthia A 2023 *JGEP.* 11 119-140. DOI: 10.4236/gep.2023.1110010
- [3] Nicholas Chia Wei Ng, Chao Li , Chenyu Wang b, Yulong Guo , Zhifei Duan , Ni Su , Shouye Yang 2023 *Journal of Geochemical Exploration.* 245 107144.
- [4] Chabaux F, Bourdon B and Riotte J 2008 *J. Environ. Elsevier.* 49–104.
- [5] Ivanovich M and Harmon R 1992, 2 ed. Oxford University Press, New York.
- [6] Claudine H, Morten B, Emma K and Alex N 2007 *EPSL.* 264 208–225.
- [7] Vasile M, Benedik L, Altitzoglou T, Spasova Y, Watjen U, Gonza'lez de Orduna R, Hult M, Beyermann M and Mihalcea I 2010 *Applied Radiation and Isotopes.* 68: 1236-1239.
- [8] El Aassy I, El Feky M, El Kasaby M, Ibrahim E, Sewef S and Attia R 2017 q *Int J Sci Eng Res* 8(1) 1135–1147.
- [9] Condomines M, Loubeau O and Patrier P 2007 *Chem. Geol.* 244 304–315.
- [10] Lehto J and Hou X 2010a *Wiley VCH Verlag GmbH & Co. KGaA,* 239-309.
- [11] Ion A, Cosac A and Victor V 2022 *Appl. Sci.* 12 <https://doi.org/10.3390/app122312363>
- [12] Amin M and Ghazala R 2014 *Chem. Tech.* 9(6) 212-217.
- [13] Harpy N, El Dabour S, Nada A, Sallam A, El Feky M and El Aassy I 2022 *J. Rad. Nucl. Appl.,* 7 (3) 41-50.
- [14] Knepper T 2003 *Trends in Analytical Chemistry* 23.
- [15] Lenhart J, Cabaniss S, MacCarthy P and Honeyman B 2000 *Radiochim. Acta.* 88 345-353.
- [16] Asselin S and Ingram J 2014 *Appl. environ. soil sci.* <http://dx.doi.org/10.1155/2014/462514>
- [17] Sun B, Zhao F, Lomb E. and McGrath S 2001 *Environ- mental Pollution* 113(2) 111–120.
- [18] Artem V, Niklas L, Paul L and Christian E. 2017 *J Solution Chem.* DOI 10.1007/s10953-017-0679-7.
- [19] Kirby H and Salutsky M 1964 The Radiochemistry of Radium, Research Division, Washington Research Center, Subcommittee on Radiochemistr, National Academy of Sciences—NaUonal Research Council.
- [20] Shapiro L and Brannock W 1962 *U.S Geol Surv Bull* 114 A.
- [21] IAEA, International Atomic Energy Agency 1987 Preparation and Certification of IAEA Gamma Spectrometry Reference Materials, RGU-1, RGTh-1 and RGK-1. International Atomic Energy Agency. Report IAEA/RL/148.
- [22] Anjos R, Veiga R, Soares T, Santos A, Aguiar J, Frasca M, Brage J, Uze da D, Mangia L, Facure A, Mosquera B, Carvalho C and Gomes P 2005 *Radiat. Meas.* 39 245–253.
- [23] Visser J and Young G 1990 *Palaeogeography, Palaeoclimatology, Palaeoecology* 81 49–57.
- [24] Odigi M and Amajor L 2009 *Chin.J. Geochem.* 28 044–054.
- [25] Taylor S and McLennan S 1985 *Blackwell, Oxford.* 312.
- [26] Harpy N, Abdel-Rahman M, Sallam A and El Dabou S 2020 *Particles and Nuclei, Letters.* 17(2) 253–259.
- [27] Adloff J, Roessler K, Recoil and Transmutation 1991 *Acta, Radiochim.* 52-53(1) 269-274.
- [28] Tuovinen H, Pohjolainen E, Vesterbacka D, Kaksonen K, Virkanen J, Solatie D, Lehto J 2016 *Environment Research.* 21 471–480.



- [29] Nada A, Imam N, El Aass, I and Ghanem A 2019 *Journal of Radioanaly Nucl. Chem*, <https://doi.org/10.1007/s10967-019-06754-9>